Published in final edited form as:
Adv Colloid Interface Sci. 2011 September 14; 167(1-2): 85–93. doi:10.1016/j.cis.2010.10.009.

Complex coacervates as a foundation for synthetic underwater adhesives

Russell J. Stewart*, **Ching Shuen Wang**, and **Hui Shao**
Department of Bioengineering University of Utah Salt Lake City, UT 84112

Abstract

Complex coacervation was proposed to play a role in the formation of the underwater bioadhesive of the Sandcastle worm (*Phragmatopoma californica*) based on the polyacidic and polybasic nature of the glue proteins and the balance of opposite charges at physiological pH. Morphological studies of the secretory system suggested the natural process does not involve complex coacervation as commonly defined. The distinction may not be important because electrostatic interactions likely play an important role in formation of the sandcastle glue. Complex coacervation has also been invoked in the formation of adhesive underwater silk fibers of caddisfly larvae and the adhesive plaques of mussels. A process similar to complex coacervation, that is, condensation and dehydration of biopolyelectrolytes through electrostatic associations, seems plausible for the caddisfly silk. This much is clear, the sandcastle glue complex coacervation model provided a valuable blueprint for the synthesis of a biomimetic, waterborne, underwater adhesive with demonstrated potential for repair of wet tissue.

Keywords

Adhesives; complex coacervates; polyelectrolytes; biomaterials; biomimicry; bioinspired

Introduction

No one has had grander notions of the biological importance of complex coacervation than Aleksandr Oparin, who in 1938 credited coacervates with a critical role in the “autogeneration of life”.[1] The authors have a more modest thesis for complex coacervation —the chemical and physical properties of coacervates make them ideal as a foundation for water-borne, underwater adhesives (fig. 1). This theory grew out of studies of the natural adhesive produced by the Sandcastle worm to glue grains of sand together into underwater sandcastles. The high charge density of the sandcastle adhesive, segregation of the opposite charges into different proteins, and balanced charge ratio at physiological pH suggested a complex coacervate could be an intermediate state in formation of the sandcastle glue.[2] Complex coacervates are concentrated, water-immiscible, aqueous fluids formed by the condensation and phase separation of oppositely charged, water-soluble polyelectrolytes. The water carrier, fluid state, water immiscibility, and density of the coacervate are ideal qualities for an adhesive that must be applied underwater. A secondary solidification

*Corresponding author rstewart@eng.utah.edu phone: 801-581-8581 fax: 801-581-8968 .

reaction, triggered by a pH change upon secretion in the case of the sandcastle glue, hardens the complex coacervate into a load bearing solid. Subsequent to the sandcastle glue model, it has been suggested that complex coacervation may play roles in the formation of the underwater adhesive silk fibers of caddisfly larvae [3] and the mussel adhesive plaque [4]. In the following, the evidence for a biochemical role of complex coacervation in each of these natural bioadhesives will be discussed, as well as the synthetic adhesives inspired by the Sandcastle worm model and their practical utility.

The Sandcastle worm

Numerous marine and freshwater invertebrates live in mineral shells. Most concentrate calcium carbonate into supersaturated solutions in cellular compartments and their shells are created to shape by controlled precipitation of calcium carbonate onto an organic matrix. The Sandcastle worm (*Phragmatopoma californica*), and related species of marine polychaetes, forego that nuisance and gather the mineral phase as preformed aggregate from its turbulent shoreside environment. It has just to produce a couple spots of glue to assemble the mineral particles into a composite tubular shell—the mineral component is nearly free. The Sandcastle worm gets its common name from the reef-like colonies that develop when new worms build their tubular dwellings on top of existing tubes.

Sandcastle Glue Structure

When a portion of a worm's tube is removed in the laboratory and building materials, like glass beads, are supplied the worm will work compulsively to repair its tube (fig. 2A).[5] The glue spots on recently placed glass beads are creamy white (fig. 2B). The glue turns tough, leathery, and progressively more reddish brown over several hours due to *o*-quinonic crosslinking (fig. 2C). The glue spots are of consistent volume, approximately 0.1 μl, and are applied only at the points where the spheres touch and at all the points of contact. From the concavity of the spots and low contact angle it is clear the glue was fluid when applied and spread on the wet surface of the glass. The worms slightly wiggle newly placed particles as if checking the set of the glue. The motion of the particles noticeably stiffens just before the worm lets go. By measuring the time the worm wiggles the particles before letting go the initial adhesive set time was estimated to be less than 30s (table 1).[6] Microscale examination by scanning electron microscopy [2] or laser scanning confocal microscopy (the glue is autofluorescent) revealed a solid foam structure with a mix of open and closed cells ranging from 0.4-6.5 μm in diameter, an overall average porosity of approximately 25%, and a steep porosity gradient from the center to the outside skin-like surface (fig. 2D).

Sandcastle Glue Composition

The laboratory-rebuilt tubes can be conveniently recovered and the proteinaceous glue digested with strong acid for subsequent amino acid and elemental analysis. Typical of structural proteins, the overall amino acid composition of the glue was dominated by just a few residues; more than 50 mol% of amino acids are glycine or serine.[7, 8] Taking into account that more than 90% of the serines are phosphorylated,[2] between 40 and 50 mol% of the total amino acids are ionizable—about 30% have phosphate sidechains and 10-20% have amine sidechains. The glue also contained a few mol% 3,4-dihydroxy-L-phenylalanine (dopa), an amino acid with a redox active catechol sidechain. The positively and negatively charged amino acids are segregated into different glue proteins, as illustrated by the representative proteins Pc3B and Pc2 (fig. 3).[8, 9] Pc3B contains serial runs of 4-14 phosphoserine (pS) residues punctuated with single tyrosine (Y) residues (fig. 3A). Pc3B is an extremely acidic protein. The tyrosines (7.7 mol%) may be hydroxylated to form dopa (fig. 3B). The MW of fully phosphorylated Pc3b is 54.8 kDa. Pc2, on the other hand, has no acidic groups, nearly 17 mol% basic residues, a pI close to 10, and 9 mol% tyrosine of

which 80% are hydroxylated to from dopa (fig. 3C).[7] Magnesium and calcium were additional major glue components identified by elemental analysis; 4-5 times more Mg was present than Ca in the set glue. The total divalent cation (Mg plus Ca) to phosphate (1500 ppm) ratio ranged from 0.6 to 1.0. Iron (30 ppm) was present at an approximately 1:5 molar ratio to dopa residues. Other transition metals were less than 3 ppm.

Sandcastle Glue Set and Cure Mechanisms

Load-bearing adhesives must solidify. The initially fluid sandcastle glue hardens into a brown, leathery, weight-bearing solid in two phases; a quick (30 sec) initial set followed by covalent curing over several hours. The initial set must be accurately timed to prevent premature hardening within the secretory pathway, yet proceed slowly enough to allow the worm time to position the particle, but not so slowly as to be inefficient. The pH differential between the regulated secretory system (pH <6) and seawater (pH >8) seemed a likely trigger. A decrease in the solubility of the conspicuous amounts of Mg/Ca and polyphosphoproteins (Pc3) in the natural adhesive could drive the initial setting reaction as a result of the pH jump accompanying secretion.[2] In support, the sparing water solubilities of the varied crystal forms of calcium phosphates are strongly pH dependent.[10, 11] Similarly, magnesium dibasic ($MgHPO_4$) and tribasic ($Mg_3(PO4)_2$) phosphates are much less soluble in water than magnesium monobasic phosphate. Nonetheless, it was unsatisfying to extrapolate from the pH dependent solubility of Ca/Mg phosphate salts to the pH dependent solubility of Ca/Mg polyphosphate. Therefore, the solubility of a synthetic polyphosphate (fig. 7A) with an average MW weight similar to Pc3B (60.4 kDa, PDI 2.5) was investigated empirically as a function of pH and the molar ratio of Mg^{2+} to phosphate side chains (fig. 4). The solubilities were investigated under their native ocean conditions of 14°C and in 470 mM NaCl. At pH 5.4, below the second pK_a of phosphate (assuming ~7.2), the synthetic polyphosphate was soluble with Mg^{2+} to PO_4 molar ratios up to 3:1. At pH 8.2, the polyphosphate was fully precipitated at ratios of 1:1 and above. Similar results were obtained with Ca^{2+} and mixtures of Ca^{2+} and Mg^{2+} (not shown). The insolubility of polyphosphate and divalent cations Mg^{2+}/Ca^{2+} at seawater pH is consistent with the pH triggered setting mechanism hypothesis. Water released during insolubilization could coalesce to form the foam cells observed in the set adhesive (fig 2D). It may also illustrate why the natural adhesive was formulated with polyphosphate rather than polycarboxylate or polysulfate; the second pK_a of phosphate falls between the internal and external pH.

The final cohesive strength is likely contributed, at least in part, by covalent crosslinking of the adhesive proteins through dopa residues, as seems to be the case with dopa-containing mussel adhesive plaque proteins.[12] The browning of the glue over several hours after secretion (fig. 2C) was indicative of oxidative conjugation between *o*-quinones and their adducts. Direct evidence of coupling between dopa and the nucleophilic thiol sidechain of cysteine was obtained by mass spectrometry of glue hydrolysates.[8] Dopa is stable at pH 5, but is oxidized into the unstable *o*-quinone more rapidly as the pH approaches the pK_{a1} (9.4) of the catechol moiety. The final cure, in principle, can be triggered entirely by the pH shift after secretion.

Sandcastle Glue Secretion

We now go backwards from the secreted glue to discuss the anatomy of the adhesive gland and the origins of the glue precursors. The adhesive gland occupies space in the first three parathoracic segments; the white bracketed region in figure 5A. The overall organization of the adhesive gland is visualized by the autofluorescence of the glue precursors within the gland and building organ, the catcher's mitt-shaped structure below the tentacles (fig. 5B). Other tissues were visualized with blue fluorescent dapi that binds nuclei. The adhesive precursors are packaged into two types of dense secretory granules, referred to as

heterogeneous and homogeneous, within distinct secretory cell types.[13] Heterogeneous granules stained black, whereas homogeneous granules stained weakly, with a reagent (van Kossa) that reacts with divalent cations (fig. 5C-E). Examination of thin, resin-embedded sections of the adhesive gland by energy dispersive x-ray spectroscopy (EDS) revealed dense substructures containing P and Mg within the heterogeneous granules, while homogeneous granules contained only background levels of these elements (fig 6). The heavily phosphorylated Pc3 protein is therefore colocalized with Mg^{2+} exclusively in the substructures of the heterogeneous granules. Using other methods, the homogeneous granules are known to contain histidine-rich proteins (unpublished). Both types of granules left their respective secretory cells (fig. 5C) in channels and traveled in segregated single-file ranks toward the building organ (fig. 5D). They arrived at the building organ intact and still unmixed (fig. 5E) and remained parked just under the surface around the entire periphery of the building organ awaiting the secretion signal. The granules were still intact when secreted from localized regions of the building organ.[14]

Complex coacervation models

The sequence of events during sandcastle glue secretion are not consistent with the initial depictions of the adhesive being secreted as a preformed, pre-mixed complex coacervate.[2, 8, 15] Instead, the oppositely charged glue proteins are secreted separately in highly concentrated granules, mixed to an unknown extent, possibly by the paddle-shaped cilia covering the building organ [14], and set-up into a load-bearing glue within 30 seconds. It seems unlikely that complex coacervation occurs post-secretion in the highly concentrated protein suspension within the short time before set. In test tubes, complex coacervates are invariably prepared by mixing comparatively dilute solutions (0.1 to 5 wt%) of oppositely charged polyelectrolytes or colloids. In fact, there is a limit to copolyelectrolyte concentration, above which complex coacervation is inhibited; 12.5 wt% in the case of whey protein and gum arabic, less in other examples [16]. Spontaneous settling of the coacervate phase can take several minutes to days. In practice, it is often accelerated by centrifugation. Without going into detail, the polyelectrolyte components [17, 18] and water [19] diffuse independently within the complex coacervate and can continue to reorganize for days after mixing. Thus, the studies of the secretion process do not support a role for complex coacervation as commonly defined and observed in practice,[20] though it is probably a minor distinction; electrostatic interactions similar in some regards to *in vitro* complex coacervation are probably at play. Additional ongoing experiments to understand the events occurring in the first few seconds after secretion may shed more light on those interactions.

Synthetic adhesive complex coacervates

Though complex coacervation may not play a role in formation of the sandcastle glue, the model inspired efforts and provided direction for copying the glue with synthetic glue protein analogs [21, 22]. The simple repetitive sequences of the glue proteins suggested they could be reasonably well replicated with poly(meth)acrylates. After all, many of the attributes of the natural adhesive proteins are fixed features of all proteins, chiral monomers and the polyamide backbone, for example. The monodisperse MW and the exact amino acid order in low complexity sequences are both consequences of templated polymerization. The blocky, repeating peptide structures reflect how nature elaborates higher MW polymers from smaller ones, by segmental gene duplication. None of these features can be assumed *a priori* to be essential for the structure and functionalities of the natural adhesive. Instead, the unique and likely most important features of the sandcastle glue are the high density of phosphate sidechains, the catechol sidechains, and segregation of opposites charges into different polymers. These features were easy to copy with inexpensive, scalable, water-soluble, synthetic poly(meth)acrylates.[21, 22] The structures of the polyphosphodopa and polyamine glue protein analogs are shown in figure 7 for comparison to the protein

structures (fig. 3). The glue protein analogs are random copolymers synthesized by free-radical polymerization. The polyphosphodopa analog typically contains 50-70 mol% phosphate sidechains and 10-20 mol% dopamine sidechains. The polyamine analog typically contains 10-20 mol% primary amine sidechains and 80-90 mol% neutral filler subunits.

When mixed at ratios of phosphate and amine sidechains and divalent cations similar to the natural glue, the analog synthetic copolymers formed colloidal polyelectrolyte complexes at low pH (fig. 8A). When the pH was adjusted upward the copolymers separated out of solution into a dense complex coacervate phase near net charge neutrality of the polyions (fig. 8B). The phase separated complex coacervate was a pipettable fluid (fig. 8C) that could be accurately delivered onto a glass surface under water without dissolving into the bath (fig. 8D). Coacervation is conceptualized molecularly, following in the footsteps of Dubin and others [16, 18, 23], as an initial electrostatic association of the analog polyelectrolytes and divalent cations into colloidal nano-complexes. At low pH, the complexes are stabilized by a net positive macroion charge compensated by counter microions (fig. 8E). The nano-complexes contain a super stoichiometric ratio of polyamine to polyphosphate due to the lower polyamine charge density. The polyamines are depicted as random coil structures that have uncharged, hydrated loops. At higher pH, as the macroionic charges approach net neutrality, the nano-complexes aggregrate with a concomitant release of microions and water, leading to partial dehydration. The polyphosphate charge density increases dramatically and the polymer chains can extend into neighboring complexes to create weaker, inter-complex associations. The polyamines remain comparatively compact because their charge density doesn't change. The circles represent potential persistence of the initial nano-complex structures in the dynamically crosslinked coacervate network. A significant degree of hydration is maintained by poor charge registration between copolyelectrolytes resulting in uncomplexed polymer loops and associated counterions. Further work is in progress to better understand the nano- and microphase structure and dynamics of the biomimetic adhesive coacervates.

The complex coacervate spread on the submerged glass surface, aided by the low interfacial tensions qualitatively evident from the flatness of the interface between the upper and lower phases (fig. 8B). Measured interfacial tensions between similar coacervates and their equilibrium phases are less than 1 mN/m [24, 25]. Adhesion to the wet glass interface is most likely mediated through the phosphate sidechains, perhaps through direct complexation with metals in the glass, or bridged through Ca^{2+} and/or Mg^{2+} to silicate groups, or other surface anions. Phosphates also adsorb tenaciously to calcium carbonate, hydroxyapatite, aluminum oxide surfaces [26], and iron oxide minerals [27]. Phosphates, in effect, are universal adhesion promoters to native wet surfaces, which may be why phosphoserines are present in the bioadhesives of mussels [28], sandcastle worms [2], sea cumbers [29], and the larval silks of caddisflies [3]. The adhesive coacervate is water-borne, in fact, mostly water by weight, so water at the interface, a significant barrier to most synthetic resins [30], readily exchanges into the watery bulk of the complex coacervate. All of these properties are ideal features for an underwater adhesive.

Analog Adhesive Set and Cure

The natural adhesive has a two-step solidification process, a quick set followed by slower covalent curing. These features were replicated in the synthetic adhesive complex coacervates.[22] An array of solutions containing varying ratios of divalent cations to phosphate sidechains and amine sidechains to phosphate sidechains were prepared at pH 5. The array established a map of polyelectrolyte and divalent cation ratios that formed complex coacervates. The same compositional grid was prepared at pH 7.4 to establish the boundaries of the coacervation space. At pH 7.4 the boundaries of the space were significantly expanded compared to the pH 5.0 boundaries. In other words, some of the

copolyelectrolytes/divalent cation ratios that were stable colloids at pH 5.0 were coacervated at pH 7.4, while some compositions that were coacervated at pH 5.0 were solid at pH 7.4. This demonstrated, in principle, that adhesive complex coacervates can be formulated with a pH-triggered hardening mechanism as predicted for the natural sandcastle glue.

The second, slower solidification step, covalent oxidative crosslinking of the adhesive into a permanent solid through dopa sidechains, was also replicated in the synthetic analog adhesive. Addition of an oxidant ($NaIO_4$) triggered crosslinking between *o*-quinones on the polyphosphodopa copolymer with primary amines on the amine copolymer (fig. 7). Bond strengths were determined by applying the adhesive complex coacervate mixed with 0.5 equivalents of $NaIO_4$ relative to dopa between a pair dripping wet polished aluminum adherends, which were then clamped and cured fully submerged in 37°C water for 24 hr. The force required to separate the lapped adherends was measured on a material testing system with the bonded adherends fully submerged in a temperature controlled water bath (fig. 9A). The bonds were never allowed to dry. The wet bond strengths of the cured complex coacervates on aluminum substrates increased as the Mg/PO_4 ratio increased with a fixed amine/PO_4 ratio (fig. 9B). The maximum average wet bond strength was 765 kPa; roughly twice the bond strength estimates of the natural sandcastle glue.[31, 32] To demonstrate the importance of coacervation, the analog copolyelectrolytes were prepared separately at high concentration (50 wt%), loaded into separate barrels of a dual syringe, and applied with $NaIO_4$ through a mixing nozzle onto Al substrates. The resulting bond strengths were less than 25% of the bond strength of the coacervated copolyelectrolytes.

One of the many challenges of developing medical adhesives is bonding in a wet physiological environment, thus providing one of the longstanding motivations for studying natural bioadhesives.[33, 34] Natural underwater adhesives are exquisitely adapted for their role in the animal's lifestyle. Since the sandcastle glue was adapted for joining wet biogenic minerals underwater it was logical to test the mimetic sandcastle glue as a bone adhesive.[35] Defects in rat calvaria were repaired with a biodegradable version of the adhesive coacervate.[22] Histological evaluation after 12 weeks demonstrated the adhesive was substantially resorbed, did not interfere with regrowth of bone into the defect, had no adverse affects on tissue adjacent to the wound site, and the inflammatory response was commensurate with normal wound healing; all of which are portents of eventual clinical utility. Of further interest to medical technologists, the complex coacervate does not wet plastic (fig. 8C,D). The comparatively higher interfacial tension with the plastic surface was apparent from the concavity of the complex coacervate surface in the narrow pipette tip (fig. 8C). This will be significant for the delivery of the adhesive through plastic catheters.

Caddisfly larvae

Caddisflies are aquatic insects that spend the majority of their life as larvae feeding below the surface of streams and lakes. They emerge only briefly as aerial adults to mate. The feeding larvae make ingenious use of sticky underwater silk to build protective structures with gathered materials. Some build stationary composite retreats assembled with silk and rocks, leaves, or sticks. Others are mobile and fashion composite armor around their soft abdomens by taping together sticks or stones with their sticky underwater silk. Caddisflies (order Trichoptera) are evolutionarily closely related to terrestrial moths and butterflies (order Lepidoptera), having diverged from a common silk-spinning terrestrial ancestor 150-200 million years ago [36]. This presented an intriguing question; what molecular adaptations of their silk allowed caddisflies to go aquatic?

Analysis of the silk proteins by energy dispersive x-ray spectroscopy, by probing with an antibody that recognizes phosphoserine, and tandem mass spectrometry, revealed that about

60% of the 15 mol% of serines in the silk were phosphorylated.[3] Moreover, the phosphoserines (pS) occurred in a repeating $(pSX)_n$ motif, where X can be one of several amino acids. By similar analyses, phosphate was not detected on H-fibroin of silk from the domesticated silkworm moth, *Bombyx mori*. Comparison of the amino acid composition of caddisfly and terrestrial moth silk (table 2) revealed another major difference; caddisfly silks had accumulated close to 15 mol% of basic residues, which are nearly absent in terrestrial silks. The gain in basic residues was mostly at the expense of alanines, which are abundant in terrestrial moth and spider silks and form β-crystalline regions that toughen the silks. The opposite charges on the caddisfly H-fibroin protein occur in alternating blocks on the highly repetitive H-fibroin protein (fig. 10). The silk also contained approximately 0.5 moles of Ca^{2+} per mole of phosphate. The answer to the molecular adaptation question seems to be, at least in part, phosphorylation of abundant serines and an accumulation of oppositely charged basic residues. What drives the underwater assembly of what would appear to be highly soluble proteins into insoluble fibers that are difficult to take apart in even harsh protein denaturing conditions?

The striking similarities to the sandcastle glue with regard to the high density and the close to balanced ratio of positive to negative charges suggested some aspect of complex coacervation could be at play in silk fiber formation. The major difference between caddisfly silk and sandcastle glue is that the charges are in alternating patches on one protein rather segregated into different proteins. Moth and spider silks have alternating hydrophilic and hydrophobic blocks. Models for silk fiber assembly in these animals posit phase separation of the amphiphilic silk H-fibroin, first into to liquid crystals,[37] or micelles,[38] in the posterior silk gland, then fibril formation when the staggered amphiphilic blocks associate laterally during stress-induced elongation of silk proteins as fibers are drawn from narrow spinnerets [39, 40]. A first model for assemble of the caddisfly silk is almost a simple word processing exercise: find and replace “amphiphilic” with “amphoteric” and “colloid or liquid crystal” with “complex coacervate” in the terrestrial silk models. High shear as the partially dehydrated caddisfly silk coacervate is drawn out of ~10 μm spinnerets [41] could induce structural reorganization of electrostatic complexes, newly exposing oppositely charged faces, association of nano-complexes into nano-fibrils, further dehydration, and insolubilization of the fiber. Although the shear-induced structural reorganization model is speculative, shear-induced phase separation of a polycationic/mixed micelle complex coacervate system provides proof-of-principle evidence [42]. At a critical shear rate around 7 s^{-1} the viscosity of the complex coacervate dropped dramatically, accompanied by macro phase separation of the coacervate. The behavior was attributed to a structural transition in the constituent nanocomplexes as they were elongated under shear that exposed new interactions sites, followed by coalescence into a more dense and dehydrated phase than the original coacervate phase.

Mussels

The best characterized natural underwater adhesive is the byssal plaque produced by marine mussels in the genus mytilus. Over the last couple decades, Herb Waite and his collaborators have teased apart the components and deciphered the complex organization of this sophisticated adhesive structure adapted to manage the vicissitudes of the mussel’s shoreline neighborhood. The plaque is comprised of at least six proteins, referred to as mussel foot proteins (mfps), distributed within the structure according to their functions (fig. 11). Mfp-1 forms a tough but extensible cuticle on the plaque and byssal thread, crosslinked through catecholate-Fe(III) complexes [43]. Mfp-1 contains 10-15 mol% dopa residues, has a basic pI around 10, and is the only protein component of the cuticle. Mfp-3 and -5, the smallest of the mfps, 7 and 9 kDa respectively, occur at the interface of plaque and substrate and hence are thought to function as adhesive primers. Mfp-3 and mfp-5 are extensively modified post-

translationally, 42 and 37% of total residues, respectively [15]. Mfp-3 contains hydroxylated arginine [44] and 10-20 mol% dopa. Mfp-5 contains phosphoserines [28] and around 30 mol % dopa. Mfp-2, -4, and -6, may form the bulk of the foamy core of the plaque in which splayed collagen fibers from the byssal thread are embedded. The adhesive plaque and byssal thread are assembled by the organized deposition of the mfps.[45] The protein components of the plaque, like the sandcastle glue, are stored in dense concentrated secretory granules that are produced and stored in different cells in different locations in the foot. The components are secreted in sequence; first, the surface primers, mfp-3 and -5. Second, the core proteins mfp-2 and -4. Last, the mfp1 cuticle protein, complexed with Fe^{3+}, as a varnish on the entire byssal thread and plaque assemble.[43]

Studies of the structural design and chemical principles of mussel adhesion have been motivated in large part by the potential of creating synthetic adhesives that bond effectively to wet surfaces. When the first mfp DNA sequences became available [46], one approach to creating a synthetic mimic of the mussel adhesive was to express recombinant mfp genes in heterologous expression hosts. Success with recombinant proteins was limited, though, generally due to poor solubility of the synthetic proteins [47]. The mfps continued to resist heterologous expression until mfp-3 and -5, the primer proteins located at the substrate interface, were fused on both ends with 6 decapeptide (AKPSYPPTYK) repeats of mfp-1, the cuticle protein [48]. The synthetic hybrid foot proteins, referred to as fp-131 or fp-151, contain ~7 kDa mfp-1 segments on each end of the 7 or 9 kDa primer proteins; the hybrid fusions are by mass more cuticle than primer. The extensive post-translational modifications of the native mfps are not executed in *E. coli* expression hosts. With post-isolation treatment with mushroom tyrosinase approximately 30% of the tyrosines in the recombinant mfps could be hydroxylated for a final 9 mol% dopa concentration [48]. The other post-translational modifications are not present.

The sandcastle glue-inspired complex coacervates prompted efforts to form complex coacervates with the mfp hybrid fusion proteins.[4] The mfp hybrids are insoluble at physiological pH so coacervation was done at pH 3.8 with hyaluronic acid (HA) at HA:fp-151 (or fp-131) ratios of 3:7. Complex coacervation of the hybrid mfps with HA led the authors to surmise that complex coacervation “might explain the mussel adhesion process” [4]. This hypothesis is more tenuous for mussels than for Sandcastle worms. It should be better reconciled with the elaborate structure, well-characterized composition, and assembly process of the mussel plaque described above. To begin with, what is the natural polyanion in the mussel adhesive analogous to the hyaluronic acid in the hybrid mfp complex coacervates? Polyelectrolytes with net opposite charges are a fundamental requirement for *complex* coacervation. The known protein components of the mussel adhesive are basic, in sharp contrast to the polyacid and polybase proteins of sandcastle glue and caddisfly silk. Acidic glycosaminoglycans are secreted from mucous glands near the tip of the foot, but their suggested function was as lubricant, sealant, and/or releasant during plaque formation [45, 49]. Second, the granules, or at least a significant proportion of the granules are still intact, when they are delivered to form the adhesive plaque.[50] Third, assembly of the plaque has been described as being analogous to “reaction injection molding”.[15, 45] The distal depression of the foot is pressed like a suction cup against a surface, then retracted somewhat to create a space and perhaps a vacuum to draw in the adhesive precursors. In other words, the mussel creates a physical space separated from the surrounding ocean in which to apply its adhesive; there is no need to invoke [4] a phase-separated complex coacervate of mfps as a means of preventing the adhesive from dispersing into the ocean. Lastly, complex coacervation of numerous random pairs of polyelectrolytes with net opposite charges have been reported, including many pairs of biological macromolecules with no natural interactions.[51] Complex coacervation is a low barrier, and by itself, is not evidence of physiological relevance. Complex coacervation of

whey protein and gum arabic,[16] for example, does not teach anything about milk cows and acacia trees.

Whether complex coacervation explains mussel adhesion or not, like sandcastle glue mimics, the hybrid mfp/HA complex coacervates may have some practical use as coatings or adhesives. Bond strengths of the HA coacervated versus uncoacervated hybrid mfps were tested on aluminum substrates in a lap shear configuration.[4] In humid conditions (not submerged), bond strengths with HA coacervated hybrid mfps were 240 kPa +/− 50%. If the bonds were air dried for 24 hrs, the *dry* bond strengths were between 3 and 4 MPa. To facilitate cell adhesion in tissue culture and other biological applications, fp-151 was fitted with an additional RGD-containing sequence at the C-terminus that binds fibronectin. The fp-151-RGD protein promoted cell attachment in culture.[52] As an HA complex coacervate, fp-151-RGD promoted pre-osteoblast cell proliferation of titanium foil, which was used as a proxy for titanium implants.[53] Curiously, the maximum cell viability was shifted toward higher HA wt% compared to the maximum extent of complex coacervation, i.e., a significant fraction of HA was not complexed in the mixtures that best promoted cell proliferation. All in all, the hybrid mfp complex coacervates may be useful as coatings if they can be prepared at reasonable cost.

Conclusions

The polyacid and polybase compositions, high charge densities, and near balance of charges at physiological pH suggest that a process similar to complex coacervation may operate during the formation of the sandcastle glue and caddisfly silk. Electrostatic interactions between concentrated water-soluble macromolecules may drive dehydration and insolubilization underwater, though not as the complex coacervation phenomenon is commonly defined and practiced in the lab, but in a richer, repeating structure-dependent manner. Whether complex coacervation plays a role in formation of natural adhesives or not, the analog adhesives based on the sandcastle glue theory will be useful. The sandcastle-inspired glue has promise as a degradable medical adhesive that may improve outcomes and reduce healthcare costs associated with repairing damaged tissues.[35]

Acknowledgments

This work was supported by grants from the NIH (EB006463) and NSF (DMR 0906014).

References

1. Oparin, AI. The Origin of Life. The Macmillan Company; London: 1938.
2. Stewart RJ, Weaver JC, Morse DE, Waite JH. J Exp Biol. 2004; 207(Pt 26):4727–4734. [PubMed: 15579565]
3. Stewart RJ, Wang CS. Biomacromolecules. 2010; 11(4):969–974. [PubMed: 20196534]
4. Lim S, Choi YS, Kang DG, Song YH, Cha HJ. Biomaterials. 2010; 31(13):3715–3722. [PubMed: 20144475]
5. Jensen RA, Morse DE. J. Comp. Physiol. B Biochem. Syst. Environ. Physiol. 1988; 158:317–324.
6. Stevens MJ, Steren RE, Hlady V, Stewart RJ. Langmuir. 2007; 23(9):5045–5049. [PubMed: 17394366]
7. Waite JH, Jensen RA, Morse DE. Biochemistry. 1992; 31(25):5733–5738. [PubMed: 1610822]
8. Zhao H, Sun C, Stewart RJ, Waite JH. J Biol Chem. 2005; 280(52):42938–42944. [PubMed: 16227622]
9. Endrizzi BJ, Stewart RJ. The Journal of Adhesion. 2009; 85(8):546–559.
10. Chow LC, Takagi S. J. Res. Natl. Inst. Stand. Technol. 2001; 106:1029–1033.

11. Kamitakahara M, Ohtsuki C, Miyazaki T. J Biomater Appl. 2008; 23(3):197–212. [PubMed: 18996965]
12. Burzio LA, Waite JH. Biochemistry. 2000; 39(36):11147–11153. [PubMed: 10998254]
13. Vovelle J. Arch. Zool. exp. gen. 1965; 106:1–187.
14. Wang, CS.; Svendsen, KK.; Stewart, RJ. Morphology of the Adhesive System in the Sandcastle Worm, Phragmatopoma californica. In: von Byern, J.; Grunwald, I., editors. Biological Adhesive Systems. Springer; New York: 2010.
15. Waite JH, Andersen NH, Jewhurst S, Sun C. The Journal of Adhesion. 2005; 81:297–317.
16. Weinbreck F, de Vries R, Schrooyen P, de Kruif CG. Biomacromolecules. 2003:293–303. [PubMed: 12625724]
17. Weinbreck F, Rollema HS, Tromp RH, de Kruif CG. Langmuir. 2004; 20:6389–6395. [PubMed: 15248727]
18. Kayitmazer AB, Bohidar HB, Mattison KW, Bose A, Sarkar J, Hashidzume A, Russo PS, Jaeger W, Dubin P. Soft Matter. 2007; 3:1064–1076.
19. Kausik R, Srivastava A, Korevaar PA, Stucky G, Waite JH, Han H. Macromolecules. 2009; 42:7404–7412. [PubMed: 20814445]
20. de Jong, HG Bungenberg. Crystallization – coacervation – flocculation. In: Kruyt, HR., editor. Colloid Science. Vol. vol. II. Elsevier Publishing Company, Inc.; 1949. p. 431-482.
21. Shao H, Bachus KN, Stewart RJ. Macromol Biosci. 2009; 9(5):464–471. [PubMed: 19040222]
22. Shao H, Stewart RJ. Adv Mater. 2010; 22(6):729–733. [PubMed: 20217779]
23. Bohidar H, Dubin PL, Majhi PR, Tribet C, Jaeger W. Biomacromolecules. 2005; 6(3):1573–1585. [PubMed: 15877380]
24. Spruijt E, Sprakel J, Stuart MA Cohen, van der Gucht J. Soft Matter. 2010; 6:172–178.
25. Hwang DS, Zeng H, Srivastava A, Krogstad DV, Tirrell M, Israelachvilia JN, Waite JH. Soft Matter. 2010; 6:p3232–3236.
26. Chang SH, Han JL, Tseng SY, Lee HY, Lin CW, Lin YC, Jeng WY, Wang AH, Wu CY, Wong CH. J Am Chem Soc. 2010; 132(38):13371–13380. [PubMed: 20822102]
27. Luengo C, Brigante M, Antelo J, Avena M. J. Colloid Interface Sci. 2006; 300:511–518. [PubMed: 16643942]
28. Waite JH, Qin X. Biochemistry. 2001; 40(9):2887–2893. [PubMed: 11258900]
29. Flammang P, Lambert A, Bailly P, Hennebert E. The Journal of Adhesion. 2009; 85:447–464.
30. Baier RE, Shafrin EG, Zisman WA. Science. 1968; 162(860):1360–1368. [PubMed: 5699651]
31. Sun C, Fantner GE, Adams J, Hansma PK, Waite JH. J Exp Biol. 2007; 210(Pt 8):1481–1488. [PubMed: 17401131]
32. Burkett JR, Wojtas JL, Cloud JL, Wilker JJ. The Journal of Adhesion. 2009; 85:601–615.
33. Despain RR, DeVries KL, Luntz RD, Williams ML. J. Dent. Res. 1973; 52(4):674–679. [PubMed: 4515845]
34. Papatheofanis BA, Ray RD. Biomat., Med. Dev., Art. Org. 1982; 10(4):247–265.
35. Winslow BD, Shao H, Stewart RJ, Tresco PA. Biomaterials. 2010
36. Yonemura N, Mita K, Tamura T, Sehnal F. J Mol Evol. 2009; 68(6):641–653. [PubMed: 19449053]
37. Vollrath F, Knight DP. Nature. 2001; 410:p541–548.
38. Jin HJ, Kaplan DL. Nature. 2003; 424(6952):1057–1061. [PubMed: 12944968]
39. Bini E, Knight DP, Kaplan DL. J Mol Biol. 2004; 335(1):27–40. [PubMed: 14659737]
40. Sehnal F, Zurovec M. Biomacromolecules. 2004; 5(3):666–674. [PubMed: 15132645]
41. Tszydel M, Sztajnowski S, Michalak M, Wrzosek H, Kowalska S, Krucińska I, Lipp-Symonowicz B. FIBRES & TEXTILES in Eastern Europe. 2009; 17(6):7–12.
42. Dubin PL, Li Y, Jaeger W. Langmuir. 2008; 24(9):4544–4549. [PubMed: 18386941]
43. Harrington MJ, Masic A, Holten-Andersen N, Waite JH, Fratzl P. Science. 2010
44. Papov VV, Diamond TV, Biemann K, Waite JH. J Biol Chem. 1995; 270(34):20183–20192. [PubMed: 7650037]

45. Waite JH. Results Probl Cell Differ. 1992; 19:27–54. [PubMed: 1289996]
46. Maugh, KJ.; Anderson, DM.; Strausberg, R.; Strausberg, SL.; McCandliss, R.; Wei, T.; Filpula, D. US. , editor. Bioadhesive coding sequences. 1990.
47. Maugh, KJ.; Anderson, DM.; Strausberg, R.; Strausberg, SL. Method of producing bioadhesive protein. In: Patent US. , editor. USA: 1993.
48. Hwang DS, Gim Y, Yoo HJ, Cha HJ. Biomaterials. 2007; 28(24):3560–3568. [PubMed: 17507090]
49. Vitellaro-Zuccarello L. Basic Appl. Histochem. 1983; 27:p103–115.
50. Tamarin A, Lewis P, Askey J. J. Morphol. 1976; 149(2):199–221. [PubMed: 933173]
51. Cornelus G, de Kruif FWaRdV. Current Opinion in Colloid & Interface Science. 2004; 9(5):340–349.
52. Hwang DS, Sim SB, Cha HJ. Biomaterials. 2007; 28(28):4039–4046. [PubMed: 17574667]
53. Hwang DS, Waite JH, Tirrell M. Biomaterials. 2010; 31(6):1080–1084. [PubMed: 19892396]

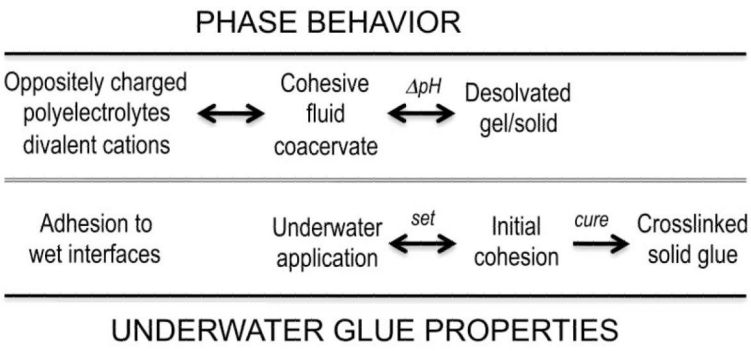

Figure 1. Complex coacervates as adhesives

The top row represents the complex coacervation and solidification of mixed polyphosphates, polyamines, and divalent cations. The bottom row connects the features of the polyelectrolyte phase behavior to the properties of an underwater glue.

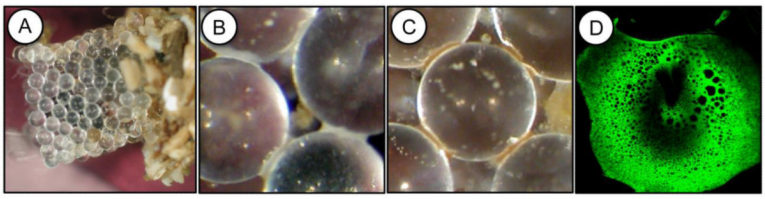

Figure 2. Sandcastle glue

A.) A tube rebuilt in captivity on top of the natural tube with 0.5 mm glass beads. B.) The recently secreted glue spots are white. The concavity of the sides and low contact angle suggested the glue was fluid when secreted and wetted the surface of the glass bead. C.) The glue spots turned brown over several hours after secretion due to oxidative crosslinking through *o*-quinones. D.) The glue was auto-fluorescent. An optical section acquired by laser scanning confocal microscopy revealed a gradient micro-foam structure.

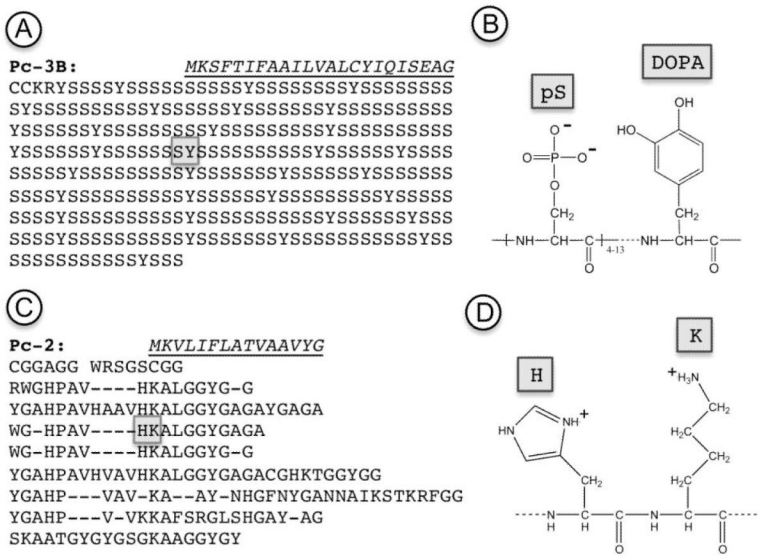

Figure 3. Representative glue protein sequences

A.) Sequence of polyacidic Pc3B. B.) The serine residues (S) are more than 95% phosphorylated on the hydroxyl sidechain. The tyrosines (Y) are hydroxylated into dopa residues. C.) Sequence of polybasic Pc2. D.) Structures of histidine (H) and lysine (K) residues with amine sidechains.

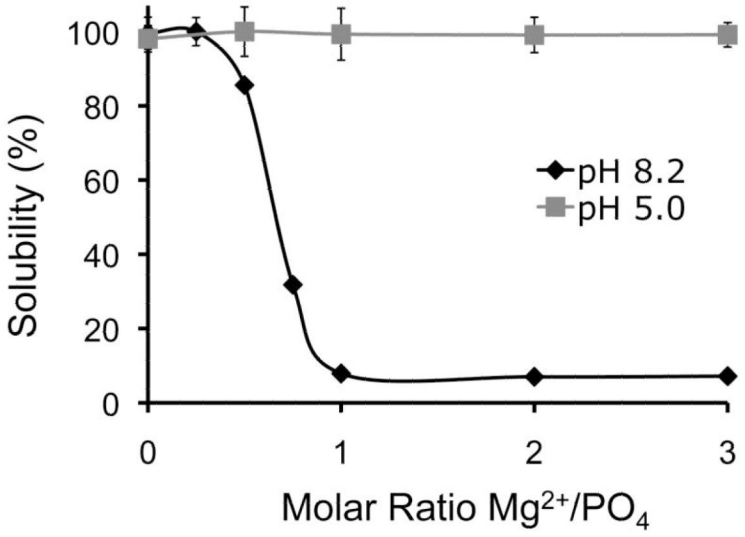

Figure 4. Synthetic polyphosphate solubility

The experimental conditions (14°C, 470 mM NaCl) simulated the Sandcastle worm's ocean environment. At approximately the pH of secretory granules (pH 5.0, gray squares) the polyphosphate (MW 60.4 kDa, PDI 2.5) was soluble at Mg^{2+} to PO_4 ratios up to 3. At the pH of the ocean (pH 8.2, black diamonds) the polyphosphate fully precipitated at a 1:1 ratio of Mg^{2+} to PO_4.

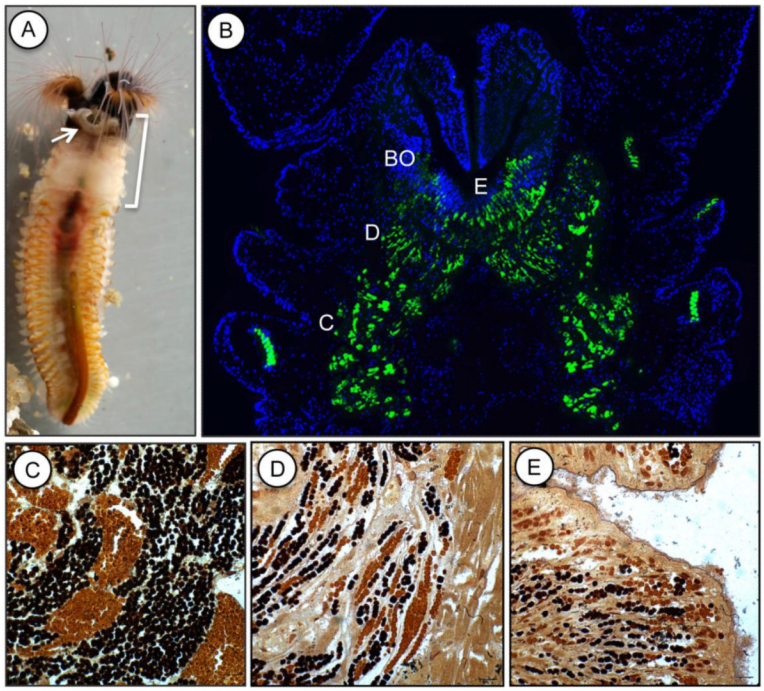

Figure 5. Structure of the adhesive gland

A.) Sandcastle worm out of its tube. The adhesive gland occurs in the first three parathoracic segments. B.) The adhesive precursors are auto-fluorescent providing an overview of the secretory system. The worm is outlined with a nuclei stain (dapi). C.) The adhesive precursors are packaged into two types of secretory granules. One type (heterogeneous) stained strongly (dark) for divalent cations. The other type (homogeneous) stained weakly. D.) The granules were transported in separate channels toward the building organ (BO). E.) The granules remained intact and unmixed when they arrived at the BO.

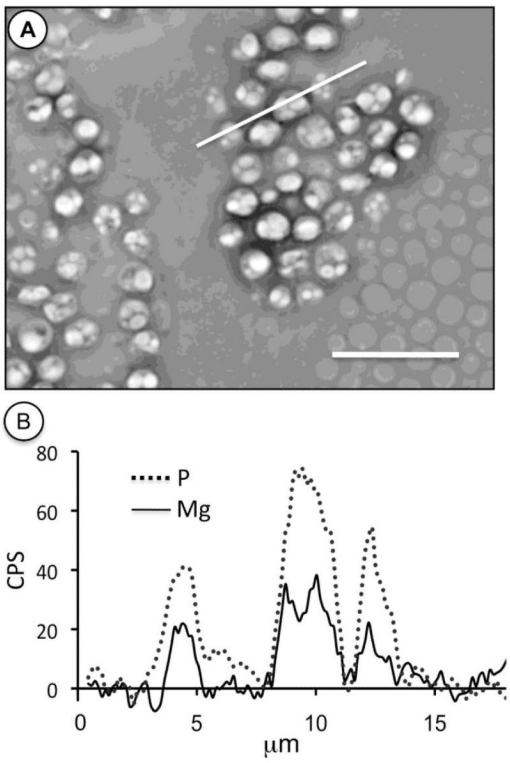

Figure 6. Elemental analysis of secretory granules by energy dispersive x-ray spectroscopy

A.) Scanning electron micrograph of a thin section of adhesive gland with a backscattered electron detector. The heterogeneous granules contain bright substructures. B.) Relative concentration of P and Mg^{2+} along the diagonal line in A. The peaks in P and Mg^{2+} are coincident with the dense substructures in the heterogeneous granules. Homogeneous granules contain background levels of P and Mg^{2+}.

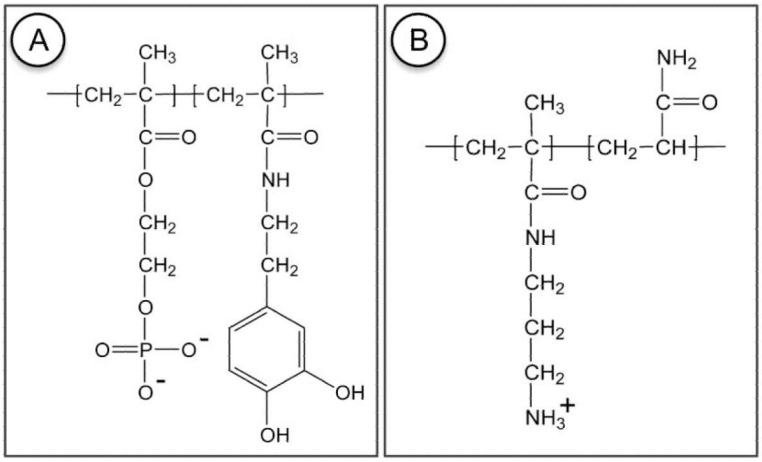

Figure 7. Synthetic analogs of glue proteins

A.) Structure of the Pc3B polymethacrylate analog copolymer. B.) Structure of the polyamine analog copolymer. The analog polymers are random copolymers synthesized by free radical polymerization.

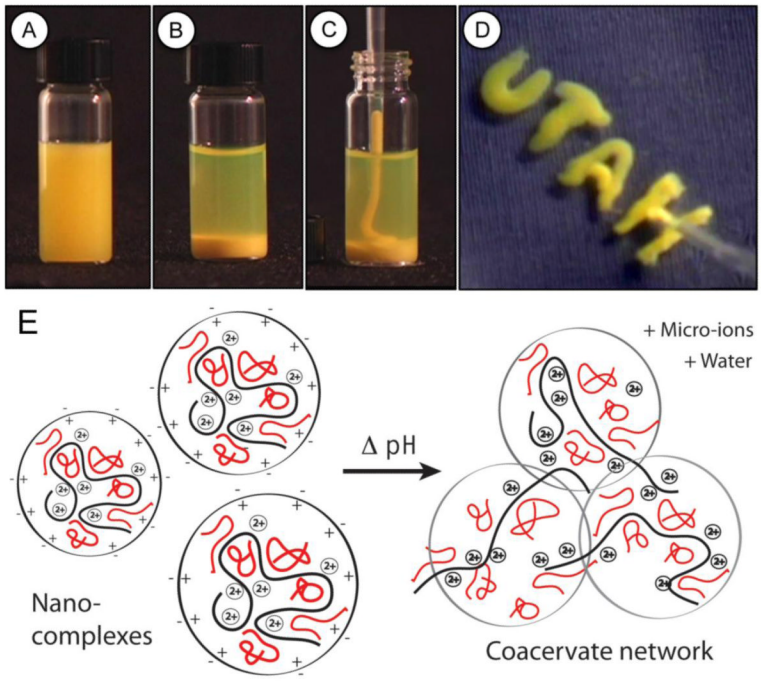

Figure 8. Complex coacervation of synthetic glue protein analogs

A.) At pH 6.0 the synthetic glue protein analogs formed a stable colloidal solution of polyelectrolyte complexes. B.) At pH 7.4 the polyelectrolytes condensed into a complex coacervate. C.) The complex coacervate was pipettable and D.) could be delivered underwater without dissolving, readily spread on the wet surface of the glass container, and did not adhere to the plastic pipette. E.) Schematic diagram of complex coacervation. Formation of the complex coacervate macrophase is preceded by formation of nanocomplexes. When the nanocomplexes are electrically neutral they associate into a liquid, interconnected network of copolyelectolyte complexes. Counter microions and water are released in the process.

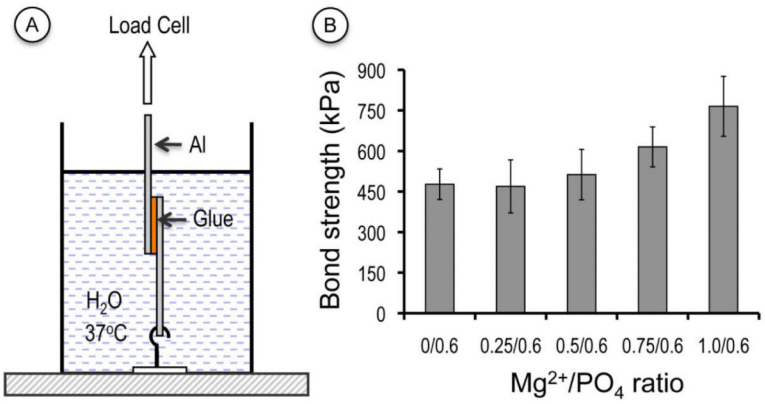

Figure 9. Bond strengths of synthetic complex coacervates

A.) Underwater test configuration with temperature controlled water bath. The bonds were formed on wet substrates and cured fully submerged in water. The bonds were never allowed to dry before testing underwater. B.) The load required to separate the bonded aluminum adherends increased as the ratio of Mg^{2+} to PO_4 increased at a fixed amine/PO4 ratio.

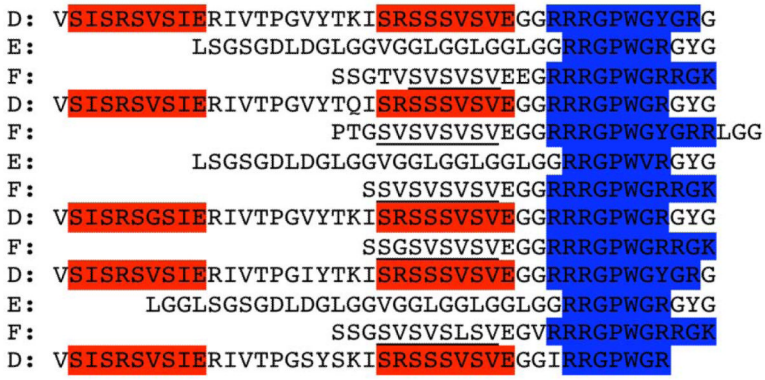

Figure 10. Repeating structure of caddisfly H-fibroin

Partial sequence (441 aa) from the C-terminus of *L. decipiens* (AB214509). The negatively charged phosphoserine blocks (gray or red) are separated by a hydrophobic region with a central proline (P) in the D repeats. A positively charged block (dark gray or blue) occurs in all three types of repeats. A $(SX)_4$ motif occurs in the F blocks but corresponding phosphorylated tryptic peptides were not found in the tandem MS spectra.

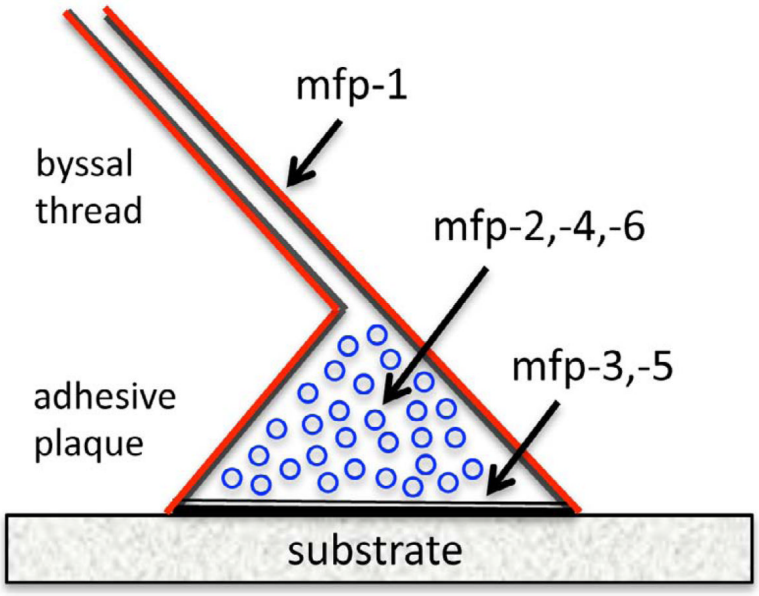

Figure 11. Distribution of foot proteins in mussel adhesive plaques

The compositional, graded structural complexity, and assembly sequence of the mussel adhesive plaque is presumably the result of adaptation to the difficult task of bonding a thread attached to its soft body to a wet hard rock. By comparison, the sandcastle worm has the simple task of externally joining together two hard mineral particles and its glue is correspondingly less complex.

Table 1

Sandcastle Glue Set Times

Substrate	Set time*
Glass beads (0.5 mm)	22.8 ± 7.5 (n = 85)
Silicon fragments	29.7 ±5.8 (n = 32)
Cortical bone fragments	23.5 ±5.3 (n = 30)

* seconds mean +/− s.d. Reproduced from [6].

Table 2

Amino acid composition of four caddisfly and two moth species.

Residue	*B. echo*[a] (mol% ± s.d.)	*L. decipiens* (mol%)	*R. obliterata* (mol%)	*H. augustipennis* (mol%)	*B. mori* (mol%)	*G. mellonella* (mol%)
Gly	20.1 ± 0.4	24.6	24.9	19.4	45.9	28.6
Ala	6.3 ± 1.1	0.4	1.9	4.5	30.3	21.3
Ser	15.4 ± 1.8	17.2	14.7	12.5	12.1	17.0
Thr	3.2 ± 0.5	2.3	1.9	2.5	0.9	3.2
Ile	3.8 ± 0.4	4.3	9.1	6.6	0.2	4.2
Leu	6.0 ± 0.6	5.0	9.5	5.4	0.1	6.6
Val	4.1 ± 0.5	12.2	5.9	9.4	1.8	6.2
Tyr	4.1 ± 0.8	2.7	1.8	6.2	5.3	0.5
Phe	1.2 ± 0.06	0.8	0.2	0.1	0.6	0.4
Pro	4.0 ± 0.3	4.8	3.3	9.6	0.3	3.8
Asx	11.7 ± 1.6	2.6	3.8	3.4	0.9	2.8
Glx	3.5 ± 0.4	3.5	4.0	3.8	0.8	2.5
Arg	8.8 ± 0.5	14.1	7.7	9.6	0.3	1.6
His	0.7 ± 0.2	0.2	6.2	2.7	0.1	0.1
Lys	4.2 ± 0.4	2.3	3.3	2.1	0.2	0.3

[a]Experimental amino acid composition from four independent analyses of *B. echo* silk. The amino acid compositions of the other species were deduced from H-fibroin sequences available in GenBank. Reproduced with permission from [3].